UNCLASSIFIED DTIC COPY MASTER COPY - FOR REPRODUCTION PURPOSES

SECURITY CLASSIFICATION OF THIS PAGE

REPORT DOCUMENTATION PAGE

(2)

AD-A222 850 C

ELECTE JUN 15 1990 S D

1a. REPORT SECURITY CLASSIFICATION	1b. RESTRICTIVE MARKINGS
2a. SECURITY CLASSIFICATION AUTHORITY	3. DISTRIBUTION/AVAILABILITY OF REPORT Approved for public release; distribution unlimited.
2b. DECLASSIFICATION/DOWNGRADING SCHEDULE	
4. PERFORMING ORGANIZATION REPORT NUMBER(S) UDR-TM-89-15	5. MONITORING ORGANIZATION REPORT NUMBER(S) ARO 26169.1-MS-A
6a. NAME OF PERFORMING ORGANIZATION University of Dayton Res. Inst.	6b. OFFICE SYMBOL (If applicable)
6c. ADDRESS (City, State, and ZIP Code) 300 College Park Dayton, Ohio 45469	7a. NAME OF MONITORING ORGANIZATION U. S. Army Research Office
	7b. ADDRESS (City, State, and ZIP Code) P. O. Box 12211 Research Triangle Park, NC 27709-2211
8a. NAME OF FUNDING/SPONSORING ORGANIZATION U. S. Army Research Office	8b. OFFICE SYMBOL (If applicable)
8c. ADDRESS (City, State, and ZIP Code) P. O. Box 12211 Research Triangle Park, NC 27709-2211	9. PROCUREMENT INSTRUMENT IDENTIFICATION NUMBER DAAL03-88-K-0203
	10. SOURCE OF FUNDING NUMBERS PROGRAM ELEMENT NO. / PROJECT NO. / TASK NO. / WORK UNIT ACCESSION NO.

11. TITLE (Include Security Classification)
Dynamic Properties of Porous B_4C

12. PERSONAL AUTHOR(S)
N.S. Brar, Z. Rosenberg, S.J. Bless

13a. TYPE OF REPORT	13b. TIME COVERED	14. DATE OF REPORT (Year, Month, Day)	15. PAGE COUNT
Interim	FROM ____ TO ____	25 January 1990	24

16. SUPPLEMENTARY NOTATION
The view, opinions and/or findings contained in this report are those of the author(s) and should not be construed as an official Department of the Army position, policy, or decision, unless so designated by other documentation.

17. COSATI CODES		
FIELD	GROUP	SUB-GROUP

18. SUBJECT TERMS (Continue on reverse if necessary and identify by block number)
Porous Ceramics, Armor ceramics, Hugoniot Elastic Limit, HEL, Boron Carbide, PMMA, Mylar, Manganin gauge (JG)

19. ABSTRACT (Continue on reverse if necessary and identify by block number)
(Boron Carbide)

The sound speed in porous B_4C was measured and predicted on the basis of a spherical void model and a penny crack model. Neither model does well for porosity exceeding 10 percent. Measured values of Hugoniot elastic limit for porous B_4C agree well with those predicted by the Steinberg's model. Measured transverse stress in the elastic range of B_4C under 1-d strain condition agrees with the predictions.

20. DISTRIBUTION/AVAILABILITY OF ABSTRACT	21. ABSTRACT SECURITY CLASSIFICATION
☒ UNCLASSIFIED/UNLIMITED ☐ SAME AS RPT. ☐ DTIC USERS	Unclassified
22a. NAME OF RESPONSIBLE INDIVIDUAL Dr. Iqbal Ahmad	22b. TELEPHONE (Include Area Code) / 22c. OFFICE SYMBOL

DD FORM 1473, 84 MAR 83 APR edition may be used until exhausted. All other editions are obsolete.

SECURITY CLASSIFICATION OF THIS PAGE
UNCLASSIFIED

TABLE OF CONTENTS

LIST OF FIGURES

LIST OF TABLES

ACKNOWLEDGEMENTS

The contribution of Z. Rosenberg to this report was supported by Dow Chemical Company under Purchase Order No. 903335. The balance of this work was sponsored by the U.S. Army Research Office under contract DAAL03-88-K-0203. The authors are grateful to Dow Chemical for making the data in Reference 1 available for additional analysis.

SECTION 1
INTRODUCTION

The dynamic properties of porous ceramics are important because ceramics are used in many lightweight armor designs. Reference 1 presents data for the dynamic properties of B_4C with porosity in the range of 0 to 15 percent, observations include variations in elastic sound speed, variations in shock strength (HEL), and measurements of shear strength.

In this report we present additional analyses of the data presented in Reference 1. We also report a few additional measurements that aid interpretation of the earlier results.

SECTION 2
MATERIALS

All porous ceramic materials tested in Reference 1 were provided by Dow Chemical Company. The ceramic plates were about 75 mm in diameter and 10.3 mm thick with faces flat within 0.001 inch. The materials were nominally the same as discussed in Reference 2 where their properties are fully disclosed.

Average densities reported in Reference 2 were nominally 85, 90, 95, and 98 percent of theoretical (2.52 g/cm^3). Porosity was uniformly distributed. The pore size was below about 5 microns. Dow measured the physical properties of specimens. Their results are summarized in Table 1.

TABLE 1

PROPERTIES OF POROUS B_4C

(FROM REFERENCE 2)

SAMPLE ID	B_4C85	B_4C90	B_4C95	B_4C98	B_4C100
Density (%)	85.7	91.7	96.0	98.8	100
Grain Size (microns)	2.09 ± 0.57	2.43 ± 0.74	2.48 ± 0.85	2.59 ± 0.75	---
Oxygen (wt. %)	0.38	0.22	0.18	0.23	---
Long. Speed (m/s)	12042 ± 117	13117 ± 140	13555 ± 171	13951 ± 59	14101
Shear Speed (m/s)	7594 ± 60	8223 ± 80	8468 ± 51	8729 ± 20	8910
Poisson's Ratio	0.17 ± 0.01	0.18 ± 0.01	0.18 ± 0.01	0.18 ± 0.01	0.17 ± 0.01
Flex. Strength (MPa)	339 ± 75	352 ± 130	414 ± 115	507 ± 92	---
Hardness (GPa)	16.5 ± 0.9	24.2 ± 0.8	34.7 ± 2.6	41.3 ± 5.4	---
Toughness (MPa$\sqrt{m}$)	2.6 ± 0.2	2.2 ± 0.2	1.9 ± 0.1	1.8 ± 0.1	---

SECTION 3
ELASTIC SOUND SPEED

The density (ρ_o) and longitudinal sound velocity (C_L) in all ceramic samples were measured in Reference 1. The data on ρ_o and C_L (from Reference 1) are summarized in Table 2 below.

TABLE 2. SUMMARY OF THE DATA ON DENSITY AND SOUND VELOCITY OF DOW B_4C CERAMICS

Ceramic Tile	Density ρ_o (g/cm^3)	Porosity (%)	Sound Velocity C_L ($mm/\mu s$)
HL1A	2.27	10	12.53
HL1C	2.26	8.97	12.51
HL1D	2.25	8.93	12.54
HL1H	2.24	8.90	12.50
HL3A	2.32	8.00	12.78
HL3B	2.35	6.70	12.83
HL2B	2.14	15	11.89
HL2C	2.11	16.30	11.83
HL4D	2.46	2.40	13.35
HL4F	2.46	2.40	13.26
HL5A	2.41	4.40	13.01
HL5C	2.39	5.20	12.97
HL5D	2.40	4.80	13.03
HL5F	2.40	4.80	13.01
Pure B_4C	2.52	----	13.42

The simplest analysis to explain the effect of porosity on elastic modulus is that of Voigt. In this analysis, it is assumed that the strain in the second phase material (the pore) is the same as in the matrix. The resulting expression for the elastic bulk modulus K is

$$K = (1 - P)\ K_s \tag{1}$$

P here is porosity, and K_s is the modulus of the matrix. The sound speed is computed from the bulk modulus (K) and shear modulus (G) using the equation

$$C_L = \sqrt{\frac{K + 4/3\ G}{\rho_o}} \tag{2}$$

G is assumed not to change with porosity.

According to Reference 3, the recommended model for porous ceramics is that of MacKenzie (Reference 4). His expressions for the dependence of K and G on porosity are

$$\frac{1}{K} = \frac{1}{K_s\ (1 - P)} + \frac{3}{4G_s}\left(\frac{P}{1 - P}\right) \tag{3}$$

$$\frac{G_s - G}{G_s} = 5\,\frac{3K_s + 4G_s}{9K_s + 8G_s}\ P \tag{4}$$

The porosity in the MacKenzie model consists of spherical voids.

Recent work on analysis of ceramics that have experienced ballistic damage have used the degraded modulus theory of Budianski (Reference 5). Budianski assumed penny-shaped cracks, and derived the expression

$$\frac{K}{K_s} = 1 - \frac{16}{9}\left(\frac{1 - \nu}{1 - 2\nu}\right) P$$

$$\nu = \nu_s \left(1 - \frac{16}{9}\ P\right) \tag{5}$$

We have compared each of these moduli with the observations summarized in Table 2. The results are shown in Figure 1. We

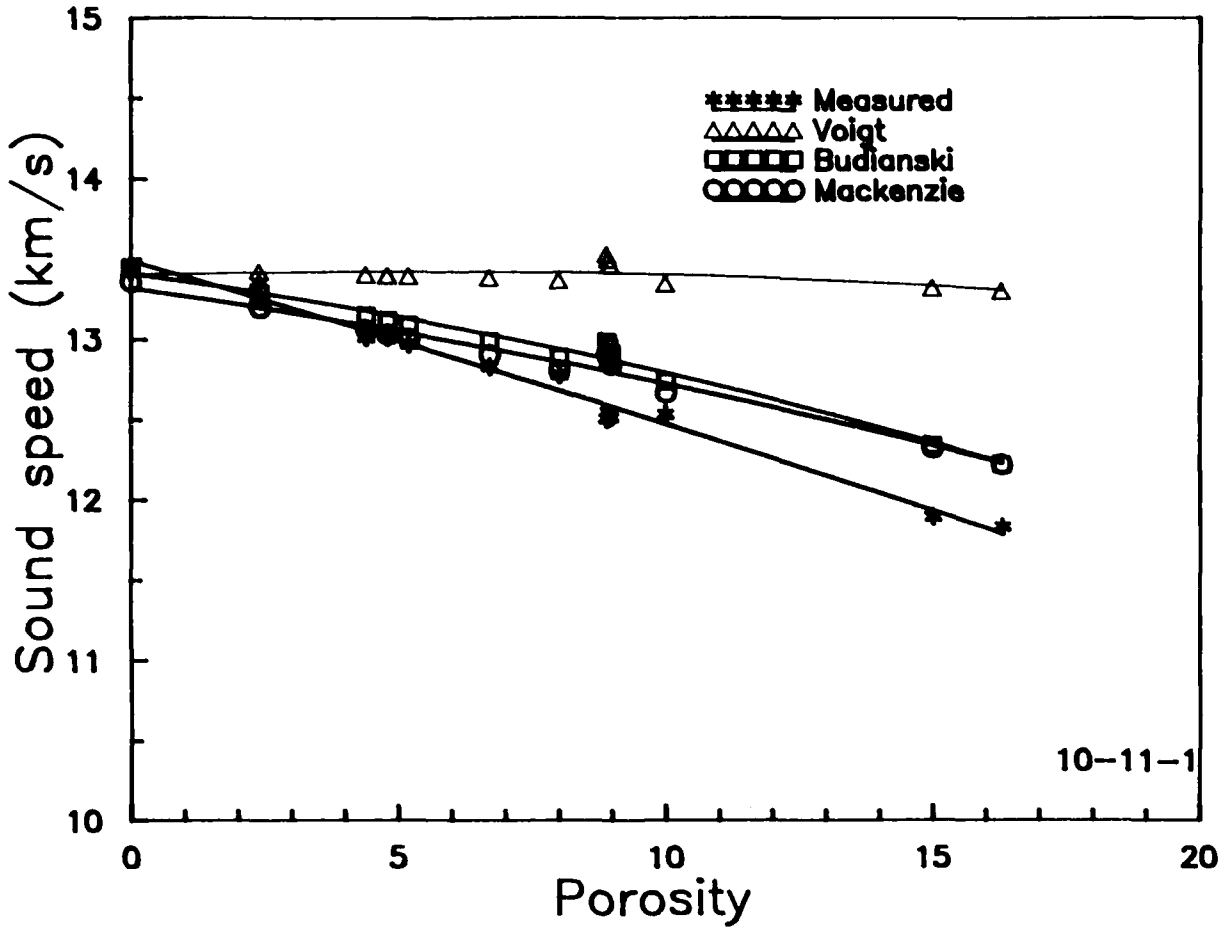

Figure 1. Comparison of Measured and Predicted Sound Speeds in Porous Boron Carbide.

see that the MacKenzie and Budianski models give very similar results, even though the assumed pore geometry is quite different. These two models also give the reasonable agreement with the data for $P < 10\%$. However, for $P > 10\%$, the agreement cannot be considered good.

SECTION 4
HEL MEASUREMENTS

Hugoniot elastic limit (HEL) values were measured in Reference 1 by placing a manganin gauge on the back of a ceramic disk backed by PMMA. The gauge was electrically insulated from the ceramic by a mylar sheet between the gauge and the ceramic. Best results were obtained with mylar thickness of 0.015 inch. A 0.5 inch thick PMMA disk was glued on the top of the gauge as shown schematically in Figure 2. Hysol epoxy was used to bond different layers in the target. Since the mechanical impedance of mylar is about the same as that of PMMA or epoxy, there were no stress reverberations in the gauge. The rise time of the stress pulse was fast enough to resolve the two wave structure resulting from elastic-plastic like behavior of the target material. The stresses recorded by the gauge are lower than those in the test material by a factor depending on the impedance ratio of the target material and PMMA. This allows the usage of the gauge for shock stresses as high as 500 kbar.

A typical gauge record is shown in Figure 3. The target in this shot (7-1285) was 90 percent dense (HLIH) and was impacted by a 4.1 mm thick copper impactor at a velocity of 1237 m/s. The two wave structure is very clear in this record which was also the case with the other HEL measurements. The value for the HEL was determined by the amplitude of the first wave at the PMMA-specimen interface (σ_1) through the well known relation:

$$HEL = \frac{Z_{SPEC} + Z_{PMMA}}{2 \times Z_{PMMA}} \cdot \sigma_1 \qquad (6)$$

where Z stands for the acoustic impedance. The accoustic impedance of the B_4C was taken as $\rho_o C_L$, using the values in Table 2. Care was taken that Z_{PMMA} was evaluated at the relevant point on the Hugoniot of PMMA. The results for the HEL

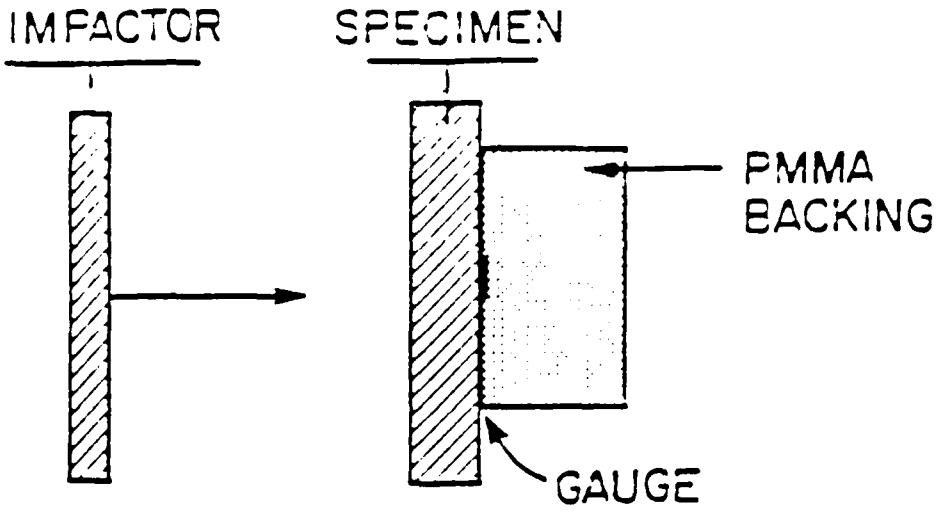

Figure 2. Schematic Representation of the Impactor and Target Assembly for HEL Measurement.

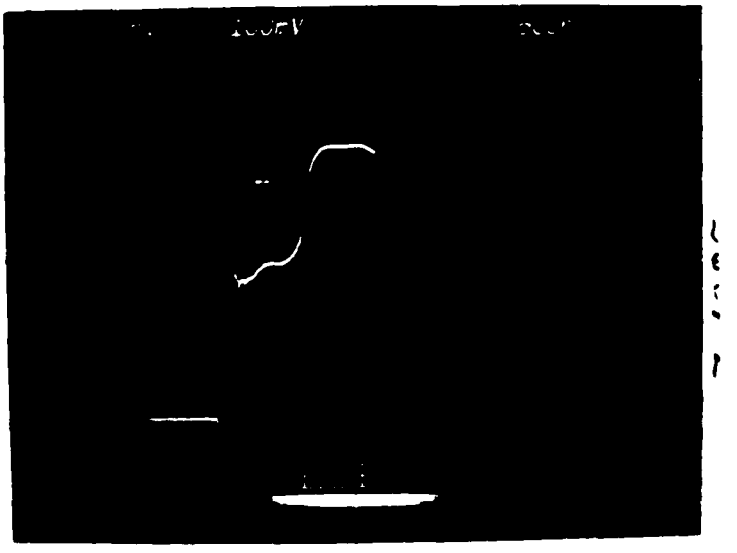

Figure 3. Oscilloscope Record of Manganin Gauge from HEL Experiment on 90 percent dense B_4C. Scales 0.5 v/div and 0.5 μs/div.

values for the different B_4C specimens are listed in Table 3, and one can clearly see the decreasing values as porosity increases.

TABLE 3. RESULTS FOR THE HEL VALUES OF THE B_4C SPECIMENS. (REFERENCE 1)

Specimen/Density		Measured σ_1 in PMMA (kb)	HEL (kb)
HL1A	2.23	36	133
HL1H	2.24	37	137
HL2C	2.11	27	96
HL4D	2.46	41	173
HL4F	2.46	40	169
HL5B	2.40	38	162
HL5F	2.40	39	164
Pure B_4C	2.52	--	194

Steinberg (Reference 6) developed a model for the influence of porosity on HEL values. Yaziv (Reference 7) successfully applied this model to data for porous BeO.

This model assumes that the change in volume between the initial state and the HEL is the same for both the fully dense and the porous material. This assumption is tantamount to assuming that up to the HEL, the stress acts on the matrix material only, i.e., it requires plastic flow to close the pores. Thus,

$$(\Delta V) = V_o - V_{HEL} = \text{const} \tag{7}$$

Writing the jump equation for stresses in the elastic range we get:

$$\sigma = \rho_o C_L^2 \cdot \epsilon = \rho_o C_L^2 \frac{\Delta V}{V_o} = \rho_o^2 C_L^2 \Delta V \tag{8}$$

from which we obtain:

$$\Delta V = \frac{\sigma_{HEL}}{Z^2} = \text{const} \tag{9}$$

This leads finally to:

$$\sigma^{P}_{HEL} = \left(\frac{Z^P}{Z^S}\right)^2 \sigma^{S}_{HEL} \tag{10}$$

where P and S stand for porous and solid material, respectively.

Using HEL = 194 kb for the fully dense B_4C we calculated the HEL of porous samples and these are compared to the measured HEL values in Table 4 and Figure 4. We find that the simple model predicts the HEL values of porous ceramics quite well.

TABLE 4. COMPARISON BETWEEN PREDICTED AND MEASURED HEL FOR POROUS B_4C CERAMIC

Sample	Porosity (%)	HEL (kbar) Measured	Calculated
HL2C	16.3	96 ± 2	106
HL1A	10	137 ± 2	137
HL1H	11.1	133 ± 2	137
HL5B	4.80	162 ± 4	165
HL5F	4.80	164 ± 4	165
HL4D	2.46	173 ± 2	183
HL4F	2.46	169 ± 2	180

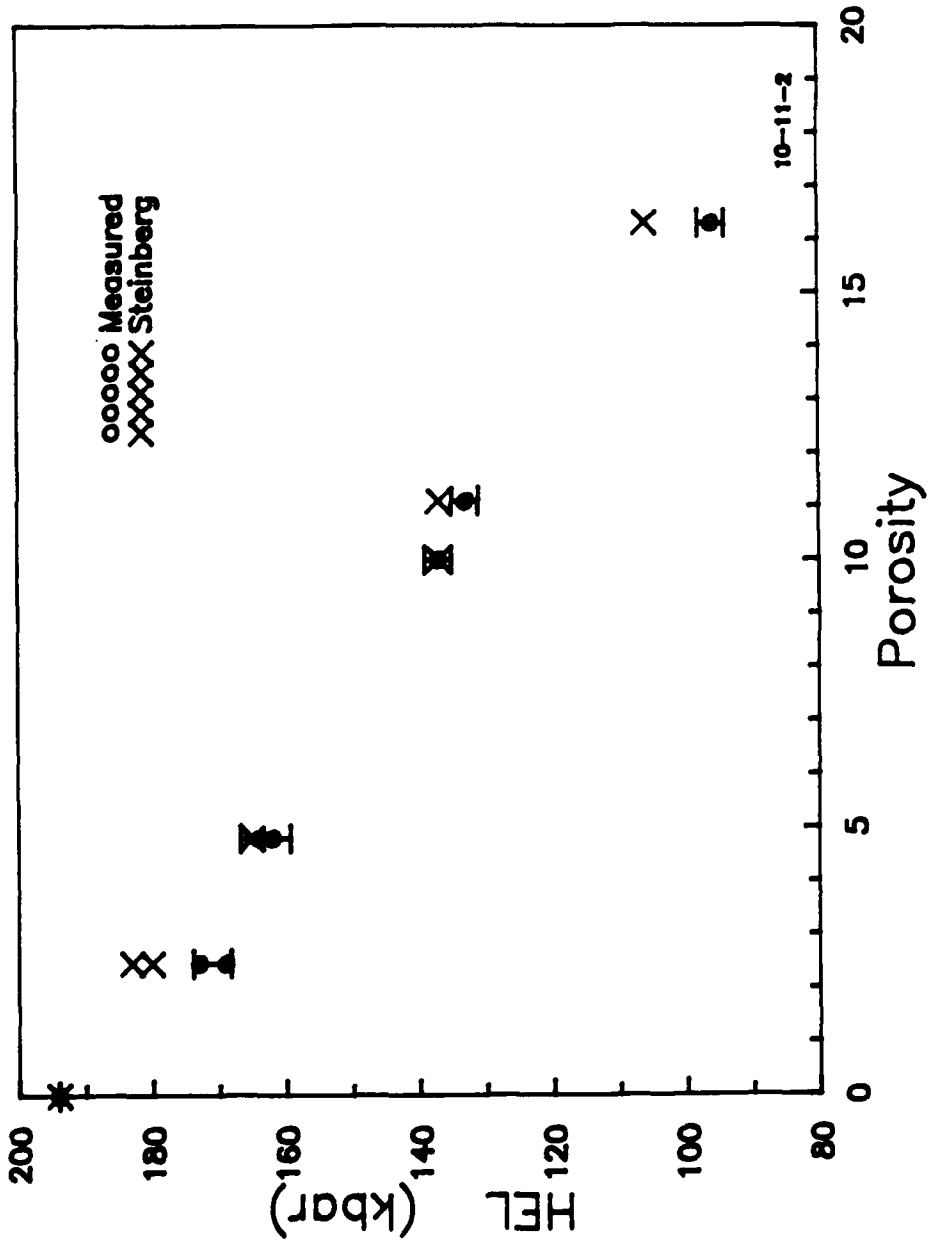

Figure 4. Measured and Predicted HEL of Porous Boron Carbide.

SECTION 5
TRANSVERSE STRESS RESULTS

The transverse gauge technique used in Reference 1 is described in Reference 8. It enables one to directly measure the shear strength of shock loaded specimens. We used this technique to measure the shear strength of shocked alumina (AD85) in Reference 9. The gauges we used in Reference 1 were narrower than the gauges used in Reference 8, in order to reduce the shock transit time through the gauge. Figure 5 shows schematically how the gauge is emplaced in the target. Thin mylar sheets (0.001 inch thick) were used in order to electrically insulate the gauge from the boron carbide specimens.

The target geometry used in Reference 1 was also similar to that used in Reference 8. The driver (front) B_4C plate was either 10 mm or 6.35 mm thick. The signals resulting from the transverse gauges showed a continuously rising transient as shown in Figure 6 from Shot 7-1311. This shot was performed on fully dense B_4C with a 10 mm thick driver plate. A copper disk (4 mm thick) was used as an impactor at a velocity of 739 m/s. In the original interpretation of the gauge records, we took the maximum gauge signal as an indicator of the maximum transverse stress.

Reconsideration of these experiments, taking into account the high sound speed in B_4C, indicates that when the driver plate was 10 mm thick, the lateral release from the edges of the flyer plate arrived at the transverse gauge only 1 μs after the plane wave; for the thinner driver plates the delay was 1.2 μs. Thus, we realized that perhaps the records such as shown in Figure 6 should be reinterpreted--the initial plateau of the signal may represent the transverse stress.

In order to check this hypothesis, we conducted an additional test in which we embedded the transverse gauge between two 10 mm thick half disks and did not use a driver plate. The shock reached the transverse gauge location in about 0.2 to 0.3 μs

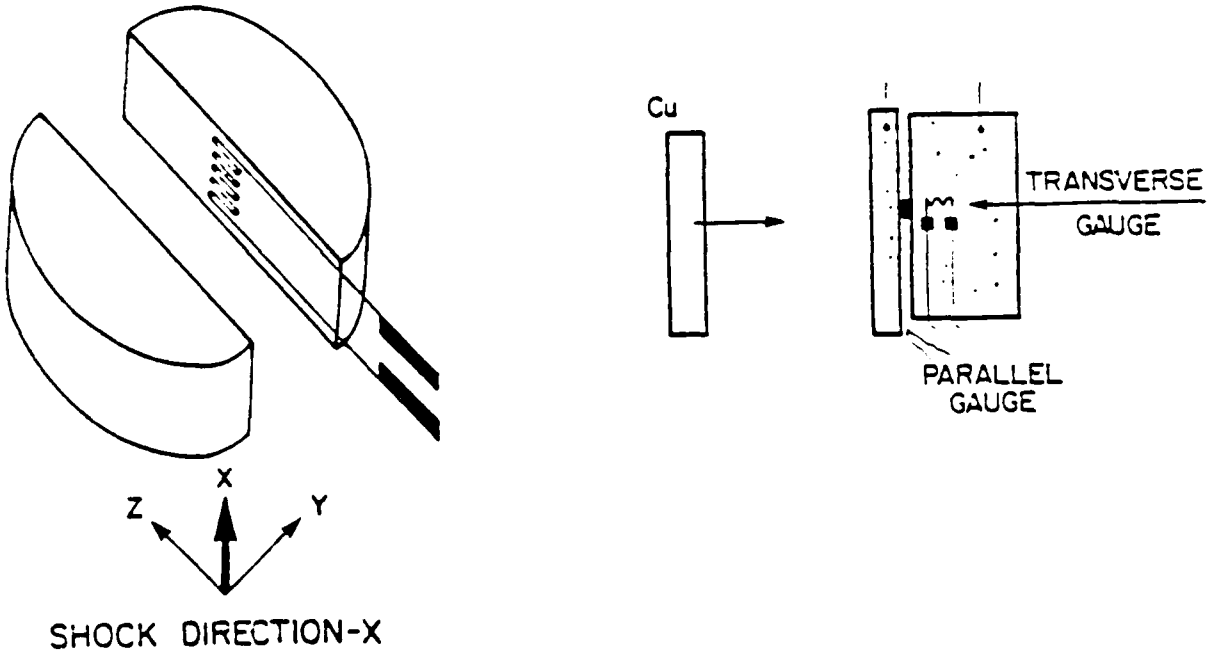

Figure 5. Schematic Representation of the Transverse Gauge Assembly.

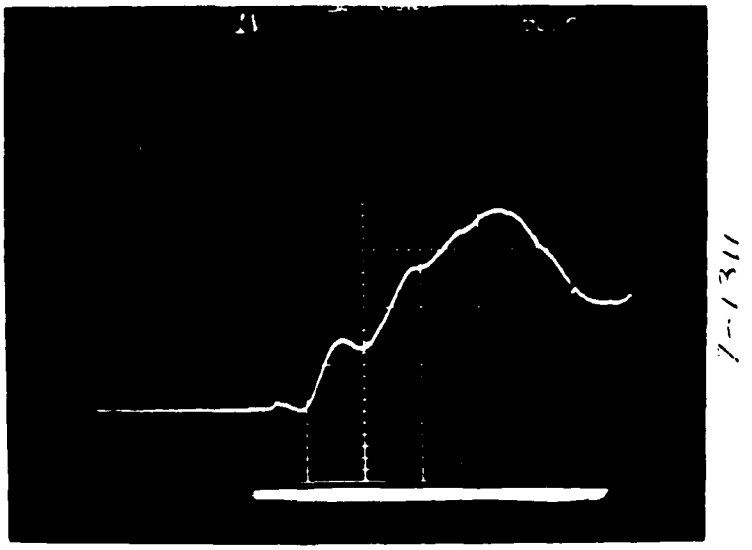

Figure 6. Oscilloscope Record of Transverse Manganin Gauge in Shot 7-1311. Scales 1.0 v/div and 0.5 μs/div.

depending upon its position with respect to the impact surface. The sample was a 10 percent porous specimen (type HL3). The disks were backed by a 12.7 mm PMMA block. The flyer plate was copper.

We noted that air bubbles appeared at the PMMA-specimen interface when this target was removed from the bonding assembly. This is a strong indication that one should be very careful about bonding B_4C specimens with epoxy resin. Roughening the surfaces may be one way to improve on this problem, using a different epoxy may be another one.

The impact velocity in this shot was 560 m/s. The transverse gauge record from this experiment is shown in Figure 7. The gauge signal becomes noisy after the arrival of the shock wave. The negative transient is probably due to collapse of air bubbles around the gauge. However, after about 0.5 μs the gauge responds in the usual manner, and one can clearly calculate the transverse stress from the flat plateau of the gauge profile. The measured peak transverse stress was 22 kbar.

The measured value can be checked for consistency. The peak shock stress in the specimen was elastic since σ_x = 105 kbar which is below the HEL. Therefore, σ_y can be calculated from σ_x using the elastic equation,

$$\sigma_y = \frac{\nu}{1 - \nu} \cdot \sigma_x = 21 \text{ kbar} \qquad (11)$$

for a Poisson's ratio of ν = 0.165 (Reference 2). The agreement between experiment and prediction is excellent in this case.

After finding excellent agreement between the measured transverse stress and the elastic prediction, we reanalysed the transverse gauge data from Reference 1, using the first stress level as a measure of σ_y. Treated in this way, the data in Reference 1 also consistently shows elastic behavior when $\sigma_x <$ HEL.

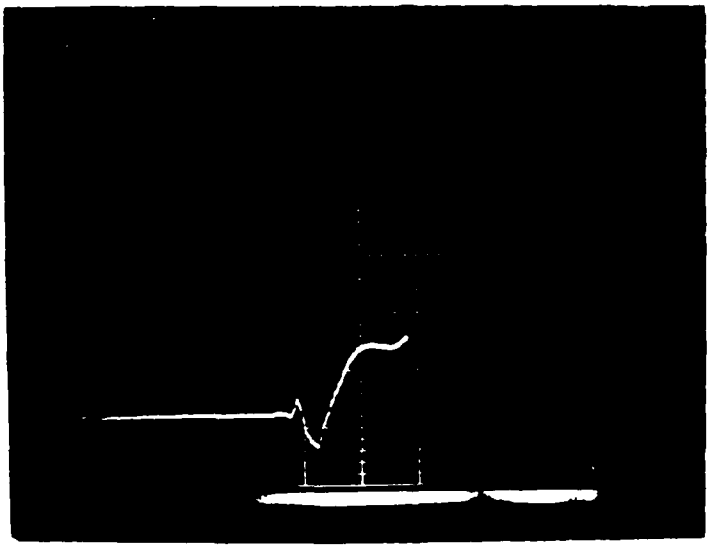

Figure 7. Oscilloscope Record of Transverse Manganin Gauge in Shot 7-1349. Scales 1.0 v/div and 0.5 μs/div.

We recommend that more experiments should be done on these materials especially above the HEL in order to determine whether the shear strength of B_4C decreases with shock stress, as some authors claim.

SECTION 6
SUMMARY

The sound speed in porous B_4C, as reported in Reference 1, can be predicted with either a spherical void model (Reference 4) or a penny crack model (Reference 5). However, neither model does well for porosity exceeding about 10 percent.

The HEL data for B_4C in Reference 1 can be predicted by the porous media model of Steinberg (Reference 6).

The transverse stress in B_4C should be measured using a target design with no driver plate. Such tests help interpretation of transverse gauge data in Reference 1. The behavior of B_4C is found to be elastic below the HEL.

REFERENCES

1. N.S. Brar, "Dynamic Response of B_4C Ceramics," University of Dayton Report, UDR-TR-89-11A, submitted to Dow Chemical, January 1990.

2. E.A. Ness, R.J. Hoffman, C.N. Haney, W. Rafaniello, and K. Moffett, "Effect of Porosity on the Ballistic Performance of Boron Carbide Armor Tiles," Fifth TACOM Armor Coordinating Conf., 7-9 March 1989, Monterey, CA.

3. W.D. Kingery, H.K. Brown, and D.R. Uhlmann, Introduction to Ceramics, Wiley & Sons, 1960.

4. K. MacKenzie, "The Elastic Constants of a Solid Containing Spherical Voids," Proc. Roy Soc. (London), B63;2-11, 1950.

5. B. Budianski and R.J. O'Connell, "Elastic Moduli of a Cracked Solid," J. Solids Structures 12;81-97, 1976.

6. D. Steinberg, "Equation of State for B_4C and BeO," LLL, Report UCID-16946, 1975.

7. D. Yaziv, S. Bless, and Z. Rosenberg, "Shock Fracture and Spall in Porous Beryllium Oxide," Proc. Int'l. Conf. Metallurgical Applications of Shock-Wave and High-Strain-Rate Phenomena, Portland, OR, 28 July-1 August 1985.

8. Z. Rosenberg and Y. Partom, "Lateral Stress Measurements in Shock Loaded Targets with Transverse Piezoresistance Gauges," J. Appl. Phys., 58:3072, 1985.

9. Z. Rosenberg, D. Yaziv, Y. Yeshurun, and S. Bless, "The Shear Strength of Shock-Loaded Alumina as Determined with Longitudinal and Transverse Gauges," J. Appl. Phys., 62:1120 1987.